Available online at www.sciencedirect.com
SCIENCE DIRECT®
Journal of Nuclear Materials 342 (2005) 68–76
journal of nuclear materials
www.elsevier.com/locate/jnucmat

Neutron displacement cross-sections for tantalum and tungsten at energies up to 1 GeV

C.H.M. Broeders [a,*], A.Yu. Konobeyev [a,b], C. Villagrasa [a]

[a] *Institut für Reaktorsicherheit, Forschungszentrum Karlsruhe GmbH, Postfach 3640, 76021 Karlsruhe, Germany*
[b] *Institute of Nuclear and Power Engineering, 249020 Obninsk, Russia*

Received 24 November 2004; accepted 9 March 2005

Abstract

The neutron displacement cross-section has been evaluated for tantalum and tungsten at energies from 10^{-5} eV up to 1 GeV. The nuclear optical model, the intranuclear cascade model combined with the pre-equilibrium and evaporation models were used for the calculations. The number of defects produced by recoil atoms nuclei in materials was calculated by the Norgett, Robinson, Torrens model and by the approach combining calculations using the binary collision approximation model and the results of the molecular dynamics simulation. The numerical calculations were done using the NJOY code, the ECIS96 code, the MCNPX code and the IOTA code.

1. Introduction

The goal of this work is the evaluation of neutron displacement cross-sections for tantalum and tungsten at energies up to 1 GeV. The significance attached to these metals as materials of advanced nuclear energy systems emphasizes the radiation damage study for both metals.

The neutron displacement cross-sections evaluated in the present work and the displacement cross-sections obtained recently for protons [1] make it possible to solve the complex problem about the radiation damage rate of tantalum and tungsten irradiated in accelerator driven systems of various design.

The first part of the work contains a brief description of methods and tools commonly used for the displacement cross-section calculation. The model calculations are compared with available experimental data and with evaluated data from ENDF/B-VI (Release 8, Section 2). The second part of the work is devoted to the displacement cross-section calculation and evaluation (Sections 3 and 4). The calculation of the primary recoil spectra was carried out using the different nuclear models, including the optical model and various intranuclear cascade evaporation models incorporated in the MCNPX code package [2]. The number of Frenkel pairs produced by the primary knock-on atoms (PKA) in materials was calculated using the NRT model [3,4] (Section 3) and by the method combining the binary collision approximation model (BCA) and the molecular dynamics method (MD) (Section 4).

* Corresponding author. Tel.: +49 7247 822484; fax: +49 7247 823718.
E-mail address: cornelis.broeders@irs.fzk.de (C.H.M. Broeders).

0022-3115/$ - see front matter © 2005 Elsevier B.V. All rights reserved.
doi:10.1016/j.jnucmat.2005.03.012

2. Brief description of models and tools used for displacement cross-section calculation

For a given neutron irradiation spectrum, the radiation damage rate is defined by the atomic displacement cross-section σ_d [1]. The calculation of the displacement cross-section consists of two relatively independent parts: the calculation of the recoil spectra $d\sigma/dT$ for all open reaction channels and the calculation of the number of displacements $N(T)$ produced by PKA's.

2.1. Nuclear models and tools used for the recoil spectra calculation

The recoil spectrum for neutron elastic scattering, $(d\sigma/dT)_{el}$ is completely defined by the angular distribution of the scattered neutrons. In the present work the nuclear optical model [5] is used for the calculation of $(d\sigma/dT)_{el}$. The comparison of the results obtained using different optical potentials is discussed in Section 2.3.

The evaluation of the recoil spectrum for reactions implies the calculation of the energy and angular distributions of the secondary particles and the residual nucleus basing on the relativistic conservation laws. In the present work, the nonelastic component of the recoil spectrum, $(d\sigma/dT)_{non}$ is calculated using various nuclear models incorporated in the MCNPX code package [2].

The popularity of MCNPX for applications is due to the combination in the package of verified and modern approaches for the simulation of nuclear interactions with media in a wide energy range. Four intranuclear cascade models are incorporated in MCNPX: the Bertini [6–9], ISABEL [10–12], CEM2k [13–19] and INCL4 [20,21] models. In the calculations discussed below the intranuclear cascade models, except the INCL4 model, were always used together with the pre-equilibrium and evaporation models. An indication on the cascade model 'Bertini' and 'ISABEL' implies also the application of the pre-compound exciton algorithm [22,23] describing the de-excitation of residual nuclei formed after the fast particle emission. 'CEM2k' always means the use of intranuclear cascade and pre-equilibrium exciton [19,24] models. The equilibrium particle emission is simulated by the Dresner model [25] and by the ABLA model [26] in the calculations carrying out using the Bertini, ISABEL and INCL4 models. The CEM2k has its own separate evaporation algorithm [19,24].

A special case is presented when the use of the intranuclear cascade model and pre-equilibrium model is chosen randomly. A selection of pure pre-equilibrium calculation is made by Monte Carlo according to the formula [27]: min(25 MeV/E, 1.0), where E is the projectile energy. If the random choice is for the intranuclear cascade calculation the pre-equilibrium model is applied only at the end of the cascade particle emission. In the MCNPX code the procedure is used only for the Bertini intranuclear cascade model. This approach is noted as 'MBP' (Mixed Bertini Pre-equilibrium model) in the present work. The calculations using the nuclear models from MCNPX were performed with a set of default parameters described in Refs. [2,27].

2.2. Comparison of calculations with available experimental data

The experimental data for recoil atom spectra are absent both for tantalum and tungsten. For this reason the comparison of the calculations and experimental data was performed for other values, which accuracy of the description is significant for the accuracy of the $d\sigma/dT$ calculation.

Fig. 1 shows the total neutron cross-section for tantalum calculated using the MCNPX code and the measured data [28–32]. The computation of the total cross-section in MCNPX is based on the approximation of results of the optical model calculation [27] and does not depend on the type of the intranuclear cascade model selected for the calculation. There is a good agreement between the MCNPX cross-sections for tantalum and the available experimental data at energies above 20 MeV. The same agreement is observed between the total cross-section calculated for tungsten and the measured data [33,34]. There is a small systematic difference between the calculated and experimental cross-sections at energies below 450 MeV.

Fig. 2 shows the neutron emission spectra for ^{184}W-irradiated 26 MeV-neutrons. The calculations were performed using different combinations of the intranuclear cascade model and evaporation model: Bertini/Dresner, Bertini/ABLA, ISABEL/Dresner, MBP/ABLA and with the CEM2k model. The measured data are from Ref. [35]. Generally, the agreement between the calculations and the experiment for ^{184}W is rather good. The good

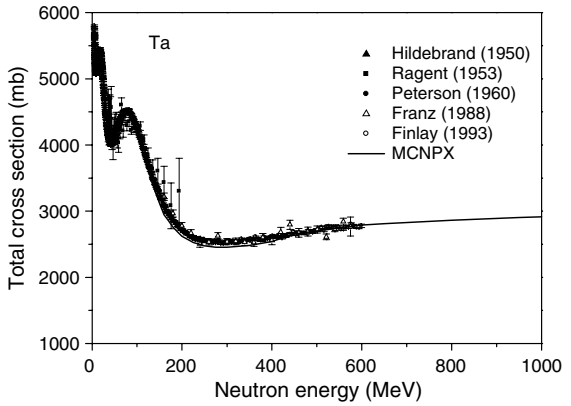

Fig. 1. Total neutron cross-section for natural tantalum calculated using the MCNPX code and measured in Refs. [28–32].

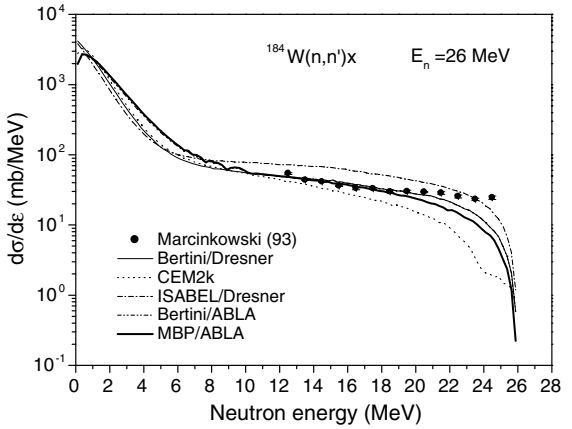

Fig. 2. Neutron emission spectra for ^{184}W irradiated with 26 MeV calculated using the different nuclear models incorporated in the MCNPX code: Bertini/Dresner (thin solid line), CEM2k (dot line), ISABEL/Dresner (dash-dot line), Bertini/ABLA (dash-dot-dot line) and MBP/ABLA (thick solid line). The measured data are from Ref. [35] (black circle).

agreement is observed also between the calculated neutron emission spectra for ^{181}Ta irradiated with 20 MeV neutrons and the measured data [36]. It is a certain success of the coupling of high energy intranuclear cascade models with pre-equilibrium exciton models implemented in MCNPX.

A double differential cross-section is another nuclear reaction characteristic of which the prediction has important significance for the accuracy of the recoil spectra calculation. Such cross-sections of neutrons emitted from ^{181}Ta irradiated with 20-MeV neutrons are shown in Fig. 3. The data for the outgoing neutron energy equal to 2.8 MeV correspond rather to the evaporation part of the ^{181}Ta(n, n′) spectrum and the data for other emission energies relate to the non-equilibrium part of the neutron spectrum. Fig. 3 shows that the best description of the experimental data is presented by the MBP/ABLA approach. The CEM2k model is also successful for the prediction of the pre-equilibrium part of the spectra at the neutron emission energy above 2.8 MeV.

The experimental information about the energy and angular distribution of the secondary particles emitted in neutron induced reaction on tantalum and tungsten above 20 MeV is limited by the data set discussed above. In this case the data for proton induced reactions can be used for the verification of methods of the calculation. Partly such verification has been made in Ref. [1]. Here the comparison of calculations with experimental data is performed for the double differential cross-sections of neutrons and protons emitted from the p + Ta reaction at the primary proton energy around 600 MeV.

Calculated and measured [37,38] distributions of neutrons and protons are plotted in Figs. 4 and 5. None of the models gives the detailed description of the experimental data. The neutron double-differential cross-sections calculated by the intranuclear cascade models are systematically lower than the measured data at various emission angles and emission energies above 50 MeV (Fig. 4).

The comparison performed for the neutron and proton angular distributions gives certain freedom at a choice of the intranuclear cascade model to obtain the neutron displacement cross-sections around 600 MeV, because none of the models shows an excellent agreement with the experimental data [37,38].

2.3. Comparison of calculations with ENDF/B-VI data

For tungsten isotopes the comparison of the calculations with the ENDF/B-VI (Release 8) data above 20 MeV can be performed directly for recoil atom spectra. Figs. 6 and 7 show the integral recoil spectra for ^{184}W irradiated with 26-MeV and 150-MeV neutrons. The spectra were taken from ENDF/B-VI (8) by summing of the individual recoil spectra for all nuclides produced in the nonelastic neutron interactions with ^{184}W and calculated using different approaches in the present work. The wide plateau in $(d\sigma/dT)_{non}$ above 0.7 MeV (Fig. 6) is formed due to the α-particle emission contribution in the recoil spectrum rather than it results from the nucleon escape, as shown in Ref. [39].

The result of the calculation for the 26-MeV neutron induced reaction (Fig. 6) is in general agreement with ENDF/B-VI. The best agreement is observed between the ENDF/B-VI data and the $(d\sigma/dT)_{non}$ spectrum calculated using the CEM2k model and the MBP model combined with the ABLA approach.

Fig. 7 shows the discrepancy between the ENDF/B-VI (8) data and the recoil spectrum calculated for 150-MeV neutron-induced reaction. The $(d\sigma/dT)_{non}$ values obtained using the different models are in a good agreement.

Due to the simplifications of the recoil data evaluation for ENDF/B-VI (8) [40] it is impossible to give an exhaustive explanation of the discrepancy between the evaluated data and the recoil spectrum calculated using the intranuclear cascade – pre-equilibrium exciton – evaporation models (Fig. 7). The discrepancy should be clarified in the further work. At present most important is the agreement between the nonelastic displacement cross-sections calculated using the nuclear models from MCNPX and obtained from ENDF/B-VI (Section 3.2).

2.4. Calculation of the number of defects produced in irradiated materials

In the present work the evaluation of neutron displacement cross-sections was performed using two different approaches for the calculation of the number of defects produced by PKA: the NRT model [3,4] and the approach [1] combining the calculations by the binary collision approximation model and the MD

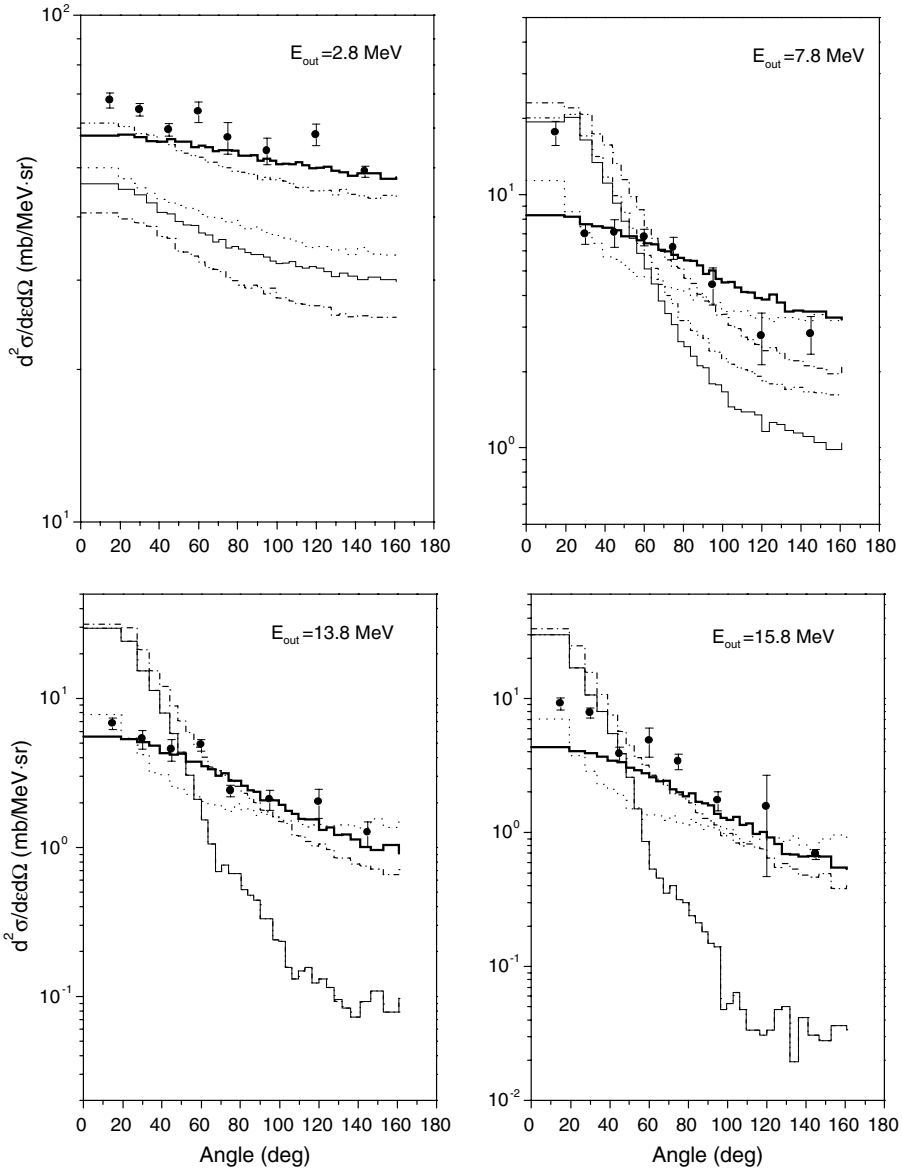

Fig. 3. Double differential cross-section of neutrons emitted with energies 2.8, 7.8, 13.8 and 15.8 MeV from the reaction of ^{181}Ta induced by 20-MeV neutrons calculated using the different nuclear models incorporated in the MCNPX code. The measured data are from Ref. [36] (black circle). See also captions in Fig. 2.

method. The effective threshold energy E_d was taken equal to 90 eV for both tantalum and tungsten [41].

3. Calculation of displacement cross-section using the NRT model

3.1. Elastic neutron scattering

In the present work the elastic displacement cross-section $\sigma_{d,el}$ has been calculated using the nuclear optical model, the neutron angular distributions from ENDF/B-VI (8) and by the MCNPX code.

The Raynal code [5] has been used for the optical model calculation. The spherical optical potentials from Refs. [42–45] and the coupled channel optical potential from Ref. [46] have been applied.

Fig. 8 shows the elastic displacement cross-section for ^{184}W calculated using the optical model and the optical potentials from Refs. [42–46], the $\sigma_{d,el}$ values obtained from the ENDF/B-VI data and the cross-sections calculated by the MCNPX code. Fig. 8 shows a scattering

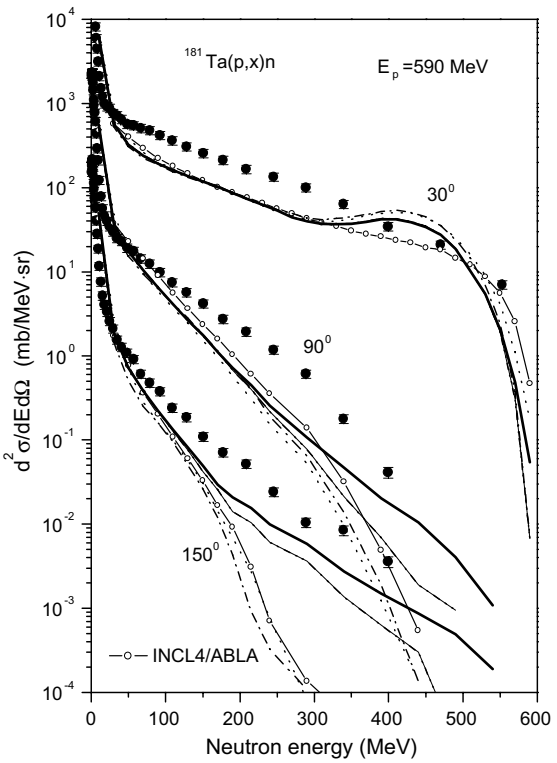

Fig. 4. Double differential cross-section of neutrons emitted from the reaction on ^{181}Ta induced by 590-MeV protons calculated using the different nuclear models incorporated in the MCNPX code: Bertini/Dresner (thin solid line), CEM2k (dot line), ISABEL/Dresner (dash-dot line), Bertini/ABLA (dash-dot-dot line), INCL4/ABLA (open circle-solid line) and MBP/ABLA (thick solid line). The results of the Bertini/Dresner and Bertini/ABLA calculations almost coincide. The measured data are from Ref. [37] (black circle).

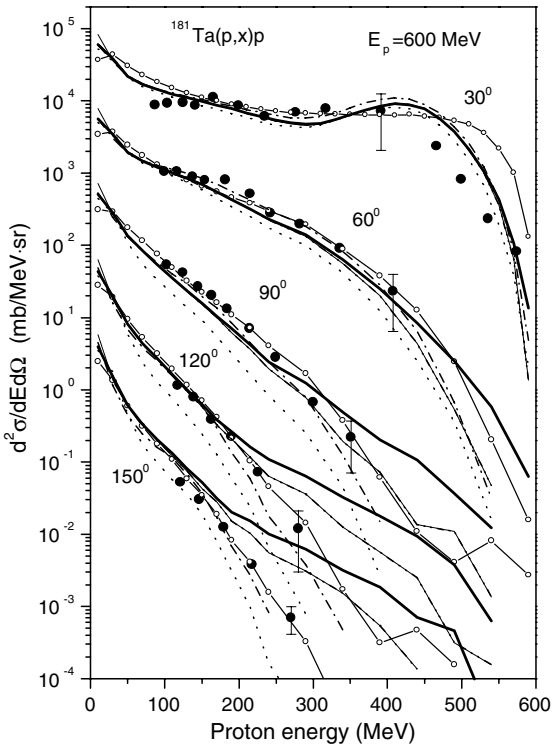

Fig. 5. Double differential cross-section of protons emitted from the reaction on ^{181}Ta induced by 600-MeV protons calculated using the different nuclear models incorporated in the MCNPX code. The measured data are from Ref. [38] (black circle). See also captions in Figs. 2 and 4.

between the elastic displacement cross-sections calculated using different sets of the optical model parameters. The agreement is observed for the coupled channel calculations with the potential from Ref. [46] and the $\sigma_{d,el}$ values ENDF/B-VI at energies up to 80 MeV. There is agreement between $\sigma_{d,el}$ calculated with the spherical optical potential of Koning, Delaroche [45] and the Walter, Guss potential [43] at energies below 50 MeV. The cross-section [45] is close to the $\sigma_{d,el}$ value obtained using the Madland potential [44] at 140–200 MeV. The ENDF/B-VI data for ^{184}W are in the agreement with the calculations performed using the Becchetti, Greenlees optical model parameters [42] at energies 20–40 MeV.

Above 50 MeV a relative uncertainty of the evaluated elastic displacement cross-section does not make a strong impact on the total displacement cross-section value, because the possible contribution of $\sigma_{d,el}$ in the total displacement cross-section does not exceed 10–13%.

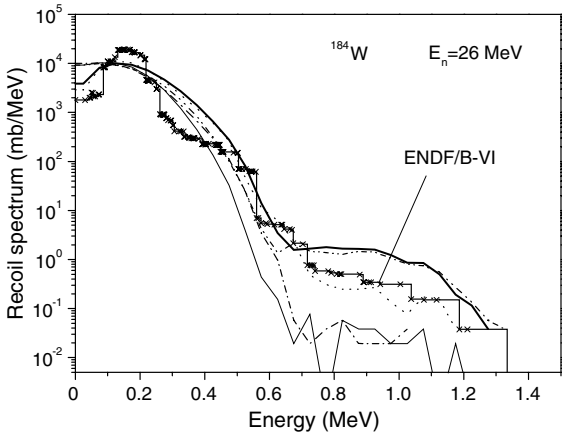

Fig. 6. Integral recoil atom spectrum for the reaction of ^{184}W induced by 26-MeV neutrons derived from the ENDF/B-VI data (cross-solid line) and calculated using the different nuclear models from MCNPX. See also captions in Figs. 2 and 4.

3.2. Nonelastic neutron interactions

The displacement cross-section related to the neutron nonelastic interaction with the nucleus, $\sigma_{d,non}$ has been

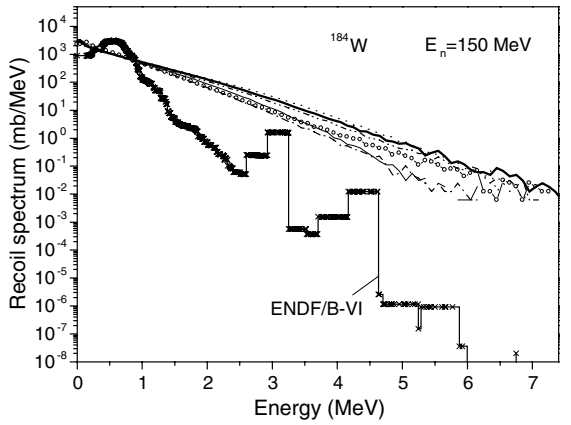

Fig. 7. Integral recoil atom spectrum for the reaction on ^{184}W induced by 150-MeV neutrons derived from the ENDF/B-VI data and calculated using the different nuclear models from MCNPX. See also captions in Figs. 2, 4 and 6.

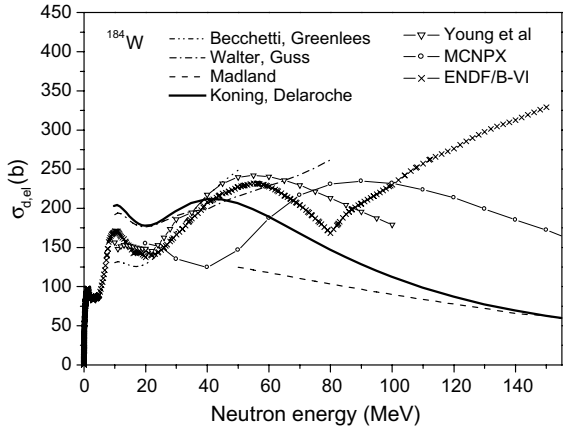

Fig. 8. Elastic displacement cross-section for ^{184}W calculated at energies below 150 MeV using the ENDF/B-VI data (cross-solid line), by the MCNPX code (open circle-solid line) and using the optical model with optical potentials of Becchetti, Greenlees [42] (dash-dot-dotted line), Walter, Guss [43] (dash-dotted line), Madland [44] (dashed line), Koning, Delaroche [45] (solid line) and Young et al [46] (open triangle-solid line).

calculated using the different models incorporated in the MCNPX code. The ENDF/B-VI (8) data were treated by the NJOY code [47].

Fig. 9 shows the $\sigma_{d,non}$ values calculated for ^{184}W at energies up to 1 GeV. A good agreement is observed between the ENDF/B-VI data and the displacement cross-sections calculated by the MBP/ABLA model at energies below 100 MeV. The ENDF/B-VI data are close to the results obtained using the Bertini/Dresner and INCL4/ABLA models at energies from 100 to 150 MeV. In general, the difference between the $\sigma_{d,non}$ values calculated

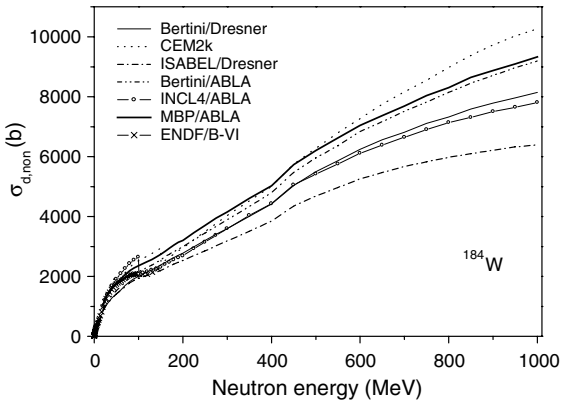

Fig. 9. Displacement cross-section for nonelastic neutron interactions with ^{184}W calculated using the ENDF/B-VI data (cross-solid line) and the different nuclear models from the MCNPX code: Bertini/Dresner (thin solid line), CEM2k (dotted line), ISABEL/Dresner (dash-dotted line), Bertini/ABLA (dash-dot-dotted line), INCL4/ABLA (open circle-solid line) and MBP/ABLA (thick solid line).

using different models is significant. The ISABEL/Dresner model gives the smallest values of the displacement cross-section comparing with other approaches. The largest values of $\sigma_{d,non}$ correspond to the results obtained by the MBP/ABLA model at energies from 150 to 450 MeV and to the CEM2k calculations at energies above 450 MeV.

As for a proton irradiation [1] the observed uncertainty in the neutron $\sigma_{d,non}$ values calculated using different nuclear models cannot be overcome at present time. It should be considered as an error of the neutron nonelastic displacement cross-section value obtained theoretically. The scattering of the results relative to the Bertini/Dresner calculations (Fig. 9) is up to 25% at the high energies.

3.3. Total displacement cross-section

The total value of the displacement cross-section σ_d was calculated as a sum of the displacement cross-sections for elastic neutron scattering $\sigma_{d,el}$ and for the neutron nonelastic interactions $\sigma_{d,non}$. The $\sigma_{d,el}$ cross-section has been calculated by the optical model with the potential of Koning, Delaroche [45] at energies 20–200 MeV. Above 200 MeV the elastic displacement cross-section has been obtained using the Madland potential [44] and by the calculation with the MCNPX code. The MBP/ABLA model showing the relative success in the description of the experimental data (Section 2.2) and the good agreement with ENDF/B-VI (8) has been used to get the $\sigma_{d,non}$ values at energies from 20 to 70 MeV. At high energies the nonelastic displacement cross-section has been calculated using the Bertini/

Dresner model. The cross-sections obtained were adjusted to the ENDF/B-VI (Release 8) data for ^{181}Ta and tungsten isotopes at 20 MeV. The evaluated total displacement cross-sections σ_d are shown in Table 1 at energies above 20 MeV. Below 20 MeV the σ_d values can be easily obtained from the ENDF/B-VI data using the NJOY code.

Table 1
Total neutron displacement cross-section evaluated for ^{181}Ta and ^{nat}W at energies up to 1 GeV

Neutron energy (MeV)	^{181}Ta	^{nat}W
20	1167	1147
22	1280	1245
24	1398	1353
26	1490	1442
28	1556	1512
30	1622	1583
35	1736	1712
40	1846	1842
45	1924	1923
50	1998	1995
55	2056	2051
60	2111	2106
65	2175	2164
70	2238	2221
75	2287	2279
80	2337	2337
85	2370	2369
90	2404	2402
95	2420	2422
100	2437	2442
110	2490	2486
120	2523	2522
130	2569	2567
140	2608	2613
150	2673	2684
160	2717	2738
170	2788	2813
180	2840	2875
190	2903	2938
200	2951	2986
225	3130	3169
250	3305	3352
275	3480	3544
300	3649	3718
350	4027	4109
400	4396	4503
450	5001	5116
500	5421	5566
550	5762	5934
600	6127	6313
650	6418	6633
700	6688	6882
750	6922	7181
800	7164	7395
850	7394	7665
900	7580	7867
950	7771	8040
1000	7937	8221

The number of defects has been calculated by the NRT model. The effective threshold displacement energy is equal to 90 eV.

4. Calculation of displacement cross-section using BCA and MD models

Detailed MD calculations providing information about the number of defects produced under irradiation, which is necessary for the calculation of displacement cross-sections, were performed up to now for tungsten only.

The number of Frenkel pairs produced in tungsten under irradiation with high energy particles has been calculated in Ref. [1] by the BCA model using the results of the MD-simulation [48]. The calculation has been done for all possible PKAs produced in the irradiation of tungsten with primary nucleons with energies up to 1 GeV. For an energetic ion moving in the material the simulation of the atomic collision was carried out using the BCA model down to a certain 'critical' energy of the ion. Below this energy the BCA calculation was stopped and the number of defects has been estimated according to the result of the MD-simulation [48]. The choice of the 'critical' energy is discussed in Ref. [1]. This procedure was carried out for all PKAs produced in atomic collision cascades. The numerical calculation was performed by the IOTA code [49]. The nuclear models and tools described in Section 3.3 were used for the recoil atom spectra calculation.

The displacement cross-sections obtained are shown in Fig. 10 at the primary neutron energies from 5 keV up to 1 GeV. For comparison the displacement cross-section calculated by the NRT model is also shown.

The ratio of the displacement cross-section calculated for natural tungsten using the BCA and MD models to

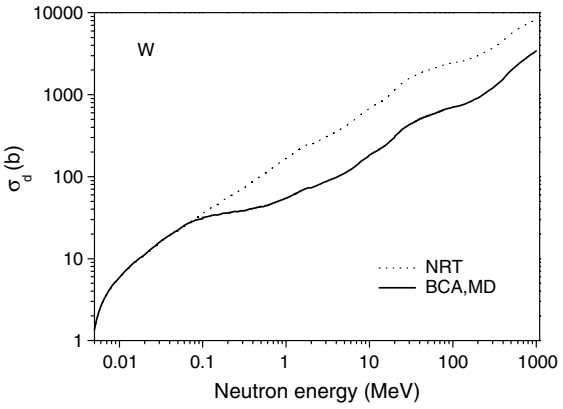

Fig. 10. Total displacement cross-section for natural tungsten irradiated with neutrons calculated using the NRT model (dash line) and the BCA and MD models (solid line) at energies from 5 keV to 1 GeV.

the cross-section obtained by the NRT model can be approximated by the following functions

$$E \leqslant 0.0657 \text{ MeV}: \quad \sigma_d^{BCA,MD}/\sigma_d^{NRT} = 1.0, \tag{1a}$$

$$0.0657 < E \leqslant 0.9 \text{ MeV}: \quad \sigma_d^{BCA,MD}/\sigma_d^{NRT} = -3.706 \cdot E^{0.13175} + 0.4825 \cdot E + 3.559, \tag{1b}$$

$$0.9 < E \leqslant 1000 \text{ MeV}: \quad \sigma_d^{BCA,MD}/\sigma_d^{NRT} = 3.279 \times 10^{-4} \cdot \ln^4(E) - 4.052 \times 10^{-3} \cdot \ln^3(E) + 2.291 \times 10^{-2} \cdot \ln^2(E) - 5.969 \times 10^{-2} \cdot \ln(E) + 0.3245, \tag{1c}$$

where E is the initial neutron energy in MeV.

Eq. (1) can be used to recover the realistic values of the displacement cross-section for natural tungsten using the cross-section obtained by the NRT model σ_d^{NRT}. The σ_d^{NRT} values are shown in Table 1 at energies above 20 MeV. Below 20 MeV the σ_d^{NRT} cross-section is prepared using the NJOY code and the ENDF/B-VI data.

For tantalum the reliable information about the energy dependence of the number of Frenkel pairs produced under the irradiation is absent. Evidently, tantalum and tungsten have similar averaged efficiency values derived from the experimental damage resistivity rates for neutron irradiation [48] (Section 2.4). Both metals have a bcc lattice, the same effective threshold displacement energy and similar nuclear properties. Nevertheless, it does not seem to be a rigorous justification of the use of Eq. (1) obtained for tungsten to get the realistic displacement cross-section for tantalum. For tantalum Eq. (1) can be used only for a crude approximate evaluation of displacement cross-section.

5. Conclusion

The displacement cross-section has been calculated for tantalum and tungsten irradiated with neutrons at energies from 10^{-5} eV up to 1 GeV.

The recoil atom spectra were calculated using the different nuclear models and tools. The nuclear optical model, the intranuclear cascade evaporation model combined with the pre-equilibrium and evaporation models was used for the calculations. The number of defects produced by residual atoms in materials was calculated by the NRT model and the approach [1] combining the BCA calculations and the results of the MD-simulation. The numerical calculations were done using the NJOY code [47], the ECIS96 code [5], the MCNPX code package [2] and the IOTA code [49].

The available neutron experimental data above 20 MeV for tantalum and tungsten were compared with the calculations carried out by various intranuclear cascade-pre-equilibrium-evaporation models from the MCNPX code package. At the initial energy around 20 MeV, the best agreement is observed between the experimental data and the calculations performed by the MBP (Mixed Bertini Pre-Equilibrium) model combined with the ABLA evaporation model.

The displacement cross-section for the elastic neutron scattering has been calculated by the optical model. For comparison, the calculation was performed using different sets of the optical model parameters [42–46]. The displacement cross-section for the nonelastic neutron interactions $\sigma_{d,non}$ has been calculated above 20 MeV by various nuclear models incorporated in MCNPX. A good agreement is observed between the ENDF/B-VI data and the displacement cross-section $\sigma_{d,non}$ calculated using the MBP/ABLA model at the energy 20 MeV for ^{181}Ta and at energies from 20 to 70 MeV for tungsten.

The total displacement cross-section σ_d has been evaluated for tantalum and tungsten at energies up to 1 GeV. The NRT model has been used for the calculation of the number of defects produced by PKAs. The cross-section σ_d was calculated below 20 MeV using the ENDF/B-VI (Release 8) data and the NJOY code. The σ_d values obtained at energies above 20 MeV are shown in Table 1.

In addition, the total displacement cross-section has been calculated for tungsten using the result of the BCA and MD-simulation. The cross-section is shown in Fig. 10. The ratio of the displacement cross-section obtained by this method to the cross-section calculated using the NRT model has been parameterized for tungsten at energies from 10^{-5} eV to 1 GeV, Eq. (1). The result obtained for tungsten can be used for a rough approximation of the realistic displacement cross-section for tantalum.

Further investigation should be done to get reliable values of the realistic displacement cross-sections for tantalum. It includes the experimental study of the damage resistivity rates under the irradiation with particles of different energy and the theoretical simulation of the damage process in tantalum.

References

[1] C.H.M. Broeders, A.Yu. Konobeyev, J. Nucl. Mater. 336 (2005) 201.
[2] J.S. Hendricks, G.W. Mckinney, L.S. Waters, T.L. Roberts, et al., MCNPX extensions, Version 2.5.0, Report LA-UR-04-0570, February 2004.
[3] M.J. Norgett, M.T. Robinson, I.M. Torrens, Nucl. Eng. Des. 33 (1975) 50.
[4] M.T. Robinson, J. Nucl. Mater. 216 (1994) 1.
[5] J. Raynal, in: Proceedings of the Specialists' Meeting on the Nucleon Nucleus Optical Model up to 200 MeV, Bruyères-le-Chatel, France, 13–15 November 1996. Available from: <http://www.nea.fr/html/science/om200/raynal.pdf>.

[6] H.W. Bertini, Phys. Rev. 131 (1963) 1801.
[7] H.W. Bertini, Phys. Rev. 188 (1969) 1711.
[8] W.A. Coleman, T.W. Armstrong, Nucleon–meson transport code NMTC, Report ORNL-4606, January 1970.
[9] T.A. Gabriel, High energy transport code HETC, Report ORNL/TM-9727;CONF-850140-2-Rev., September 1985.
[10] Y. Yariv, Z. Fraenkel, Phys. Rev. C 20 (1979) 2227.
[11] Y. Yariv, Z. Fraenkel, Phys. Rev. C 24 (1981) 488.
[12] K. Chen, Z. Fraenkel, G. Friedlander, J.R. Grover, J.M. Miller, Y. Shimamoto, Phys. Rev. 166 (1968) 949.
[13] A.S. Iljinov, A code for intranuclear cascade calculation in the energy range <5 GeV, JINR Report B1-4-5478, Dubna, 1970.
[14] V.S. Barashenkov, V.D. Toneev, Interaction of High Energy Particles and Nuclei with Atomic Nuclei, Atomizdat, Moscow, 1972.
[15] K.K. Gudima, S.G. Mashnik, V.D. Toneev, Nucl. Phys. A 401 (1983) 329.
[16] S.G. Mashnik, Nucl. Phys. A 568 (1994) 703.
[17] S.G. Mashnik, A.J. Sierk, O. Bersillon, T. Gabriel, Nucl. Instrum. and Meth. A 414 (1998) 68, Report LA-UR-97-2905, 1997. Available from: <http://t2.lanl.gov/publications/publications.html>.
[18] S.G. Mashnik, R.J. Peterson, A.J. Sierk, M.R. Braunstein, Phys. Rev. C 61 (2000) 034601.
[19] S.G. Mashnik, K.K. Gudima, I.V. Moskalenko, R.E. Prael, A.J. Sierk, Adv. Space Res. 34 (2004) 1288.
[20] J. Cugnon, C. Volant, S. Vuillier, Nucl. Phys. A 620 (1997) 475.
[21] A. Boudard, J. Cugnon, S. Leray, C. Volant, Phys. Rev. C 66 (2002) 044615.
[22] R.E. Prael, M. Bozoian, Adaptation of the multistage preequilibrium model for the Monte Carlo method (I), Report LA-UR-88-3238, 1998.
[23] R.E. Prael, A review of physics models in the LAHETTM code, Report LA-UR-94-1817, Los Alamos National Laboratory, 1994.
[24] International codes and model intercomparison for intermediate energy activation yields, Report NSC/DOC(97)-1, January 1997. Available from: <http://www.nea.fr/html/science/docs/1997/nsc-doc97-1/append3.pdf>.
[25] L. Dresner, EVAP – A Fortran program for calculating the evaporation of various particles from excited compound nuclei, Report ORNL-TM-196, 1961.
[26] A.R. Junghans, M. De Jong, H.-G. Clerc, A.V. Ignatyuk, G.A. Kudyaev, K.-H. Schmidt, Nucl. Phys. A 629 (1998) 635.
[27] L.S. Waters (Ed.), MCNPX^{TM} User's Manual, Version 2.3.0, Report LA-UR-02-2607, 2002.
[28] R.H. Hildebrand, C.E. Leith, Phys. Rev. 80 (1950) 842.
[29] B. Ragent, The variation of high-energy total neutron cross sections with energy, Report UCRL-2337, 1953.
[30] J.M. Peterson, A. Bratenahl, J.P. Stoering, Phys. Rev. 120 (1960) 521.
[31] J. Franz, H.P. Grotz, L. Lehmann, E. Roessle, H. Schmitt, L. Schmitt, Nucl. Phys. A 490 (1988) 667.
[32] R.W. Finlay, W.P. Abfalterer, G. Fink, E. Montei, T. Adami, P.W. Lisowski, G.L. Morgan, R.C. Haight, Phys. Rev. C 47 (1993) 237.
[33] V.P. Dzhelepov, V.I. Satarov, B.M. Golovin, Z. Eksperiment. Teoret. Fiz. 29 (1955) 369, English translation: Soviet Physics – JETP 2 (1956) 349.
[34] W.P. Abfalterer, F.B. Bateman, F.S. Dietrich, R.W. Finlay, R.C. Haight, G.L. Morgan, Phys. Rev. C 63 (2001) 044608.
[35] A. Marcinkowski, J. Rapaport, R.W. Finlay, C. Brient, M.B. Chadwick, Nucl. Phys. A 561 (1993) 387.
[36] A. Marcinkowski, R.W. Finlay, J. Rapaport, P.E. Hodgson, M.B. Chadwick, Nucl. Phys. A 501 (1989) 1.
[37] D. Filges, S. Cierjacks, Y. Hino, T.W. Armstrong, P. Cloth, Validation of the intra-nuclear cascade evaporation model for particle production, Report KFK-3779, 1984.
[38] K.R. Cordell, S.T. Thornton, L.C. Dennis, R.R. Doering, R.L. Parks, T.C. Schweizer, Nucl. Phys. A 352 (1981) 485.
[39] E. Daum, U. Fischer, A.Yu. Konobeyev, Yu.A. Korovin, V.P. Lunev, U. von Möllendorff, P.E. Pereslavtsev, M. Sokcic-Kostic, A.Yu. Stankovsky, P.P.H. Wilson, D. Woll, Neutronics of the high flux test region of the international fusion materials irradiation facility, Report FZKA 5868, June 1997.
[40] M.B. Chadwick, P.G. Young, R.E. MacFarlane, A.J. Koning, in: Proceedings of the 2nd International Conference on Accelerator Driven Transmutation Technology and Applications, Kalmar, Sweden, June 3–7, 1996, p. 483.
[41] C.H.M. Broeders, A.Yu. Konobeyev, J. Nucl. Mater. 328 (2004) 197.
[42] F.D. Becchetti Jr, G.W. Greenlees, Phys. Rev. 182 (1969) 1190, Available from: <http://www-nds.iaea.org/RIPL-2/>.
[43] R.L. Walter, P.P. Guss. Available from: <http://www-nds.iaea.org/RIPL-2/>.
[44] D.G. Madland, in: Proceedings of the Specialists' Meeting on the nucleon–nucleus optical model up to 200 MeV, Bruyeres-le-Chatel, France, 13–15 November 1996, Report LA-UR-97-0306, 1985. Text is available at <http://arxiv.org/abs/nucl-th/9702035>. Available from: <http://www-nds.iaea.org/RIPL-2/>.
[45] A.J. Koning, J.P. Delaroche, Nucl. Phys. A 713 (2003) 231, Available from: http://www-nds.iaea.org/RIPL-2/.
[46] P.G. Young, E.D. Arthur, M. Bozian, T.R. England, G.M. Hale, R.J. Labauve, R.C. Little, et al., Report LA-11753-MS, 1990; Report LA-8630-PR, 1980, p. 2. Available from: <http://www-nds.iaea.org/RIPL-2/>.
[47] R.E. MacFarlane, NJOY99.0: Code System for Producing Pointwise and Multigroup Neutron and Photon Cross Sections from ENDF/B Data, RSICC Code Package PSR-480.
[48] M.J. Caturla, T. Diaz De La Rubia, M. Victoria, R.K. Corzine, M.R. James, G.A. Greene, J. Nucl. Mater. 296 (2001) 90.
[49] C.H.M. Broeders, A.Yu. Konobeyev, K. Voukelatou, IOTA – a code to study ion transport and radiation damage in composite materials, Report FZKA 6984, 2004.